Title

Measurement of Infiltration Using Fan Pressurization and Weather Data

Authors

Sherman, M H

Grimsrud, D T

Publication Date

1980-10-01

Lawrence Berkeley Laboratory
UNIVERSITY OF CALIFORNIA

ENERGY & ENVIRONMENT DIVISION

Presented at the First Symposium of the Air Infiltration Centre on Instrumentation and Measurement Techniques, Windsor, England, October 6-8, 1980

MEASUREMENT OF INFILTRATION USING FAN PRESSURIZATION AND WEATHER DATA

M.H. Sherman and D.T. Grimsrud

October 1980

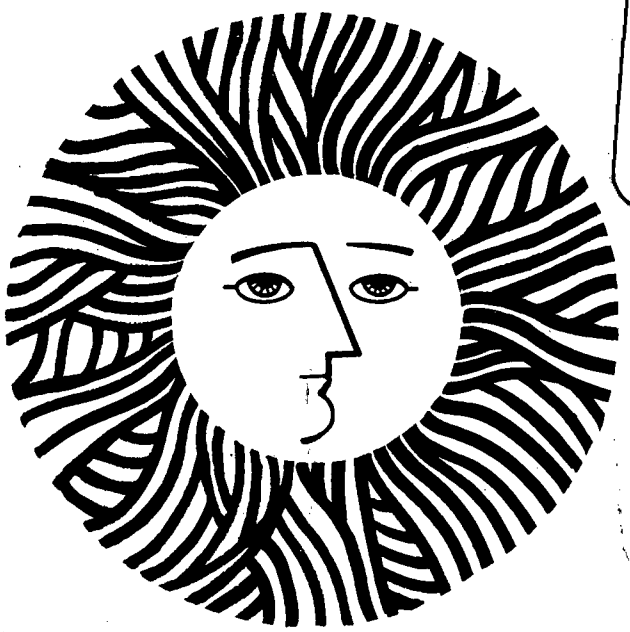

Prepared for the U.S. Department of Energy under Contract W-7405-ENG-48

DISCLAIMER

Measurement of Infiltration Using Fan Pressurization and Weather Data

M.H. Sherman and D.T. Grimsrud

Energy and Environment Division
Lawrence Berkeley Laboratory
University of California
Berkeley, Ca. 94720

In the past, expensive instrumentation, usually involving tracer gases, has been required to measure air infiltration; in this paper a technique using the results of fan pressurization and weather data to calculate infiltration is presented. The geometry, leakage distribution, and terrain and shielding classes are combined into two reduced parameters which allow direct comparison of wind-induced and temperature-induced infiltration. Using these two parameters and the total leakage area of the structure (which is found from fan pressurization) the infiltration can be calculated for any weather condition. Experimental results from fifteen different sites is presented for comparison with theoretical predictions.

Keywords: infiltration, pressurization, leakage, modeling, correlation, weather, terrain, shielding

---

This work was funded by the Assistant Secretary for Conservation and Solar Applications Buildings Division Office of Buildings and Community Systems, of the U.S. Department of Energy under contract No. W-7405-Eng-48.

INTRODUCTION

Because infiltration is a primary source of energy loss in residences, understanding the infiltration process is critical to any residential conservation program. Yet we are far more capable of calculating losses due to conduction than losses due to infiltration. Several explanations for this disparity can be cited. First, conduction losses are more easily calculated because the heat transfer is proportional to the temperature difference and does not depend strongly on any other driving force. Infiltration, on the other hand, depends on the interior-exterior pressure difference but is not simply proportional to it. Furthermore, the driving pressure is caused by uncorrelated physical effects (wind speed and temperature difference). Second, conduction losses can be characterized by means of one parameter, thermal resistance, whereas infiltration, until now, has had no equivalent quantity.

Many attempts at infiltration modeling have been made in the past; but the results of such models have been very disappointing. Virtually all of the previous models have been either inaccurate or site-specific; the only exception is a class of detailed models requiring such a large amount of information that they are impractical to use as predictive tools. Listed below are the types of models currently in use:

- Constant Rate: The constant-rate model is the simplest model of all; it assumes that the infiltration rate (i.e., the number of volumes per unit time) is a constant, independent of all other factors (e.g., weather, leakage, occupancy, size, etc.). It is this model that most large computer programs currently use for calculating building performance. Understandably, a strong appeal of this model is precisely because the only information required to calculate infiltration is infiltration. In the absence of a better model, designers and engineers have simply been specifying the infiltration rate in their designs without having any idea whether their guesses approach reality. It's also true that in the past the only need for calculating infiltration was to size equipment (e.g., heating plant, air-handling systems etc.) and this "zeroth" order approach was sufficient. Now that energy conservation and, with it, indoor air quality have become important issues, this type of model is clearly inadequate.

- Air-Change Method: This model represents an attempt to estimate the total infiltration by modifying the constant-rate method on a room-to-room basis. Each room is assumed to have a constant infiltration rate that is based on the number of existing exterior doors and

windows; studies made on small buildings yield the values for this rate. Again, no attempt is made to measure or estimate either the leakiness of the envelope or the driving pressures across it.

Crack Method: The crack method, the first real attempt to estimate the leakage of the building envelope, assumes that the infiltration will be proportional to the "crackage" and some pressure raised to an arbitrary power:

$$Q = C \Delta P^n \qquad (1)$$

where

Q is the infiltration,

C is the crackage,

ΔP is a "design pressure drop" and

n is the exponent.

The exponent is usually assumed to be equal to 0.65 and the pressure drop is a single number calculated by estimating the pressure due to the difference in buoyancy between inside and outside air, and adding to that value the pressure caused by the wind. The crackage is calculated by finding the length of crack associated with each door and window in the envelope, multiplying it by a tabulated quantity dependent on the type of penetration (e.g., double-hung window, wall-frame leaks around masonry, etc.). Although this method does attempt to use weather information to estimate the infiltration, unfortunately, since it uses only design pressures, it cannot be used to estimate instantaneous infiltration, or even long-term average infiltration — only design infiltration. Furthermore, the estimation of crackage does not take into account installation of fenestration, etc. It has been found that installation practices and aging can each change the leakage behavior by a factor of two.

The above two methods have been used by designers and, until recently, have been the ASHRAE standard methods used to size equipment as well as to estimate infiltration. A review of the ASHRAE models has been prepared by J. Jansen.[1]

- Linear Regression Techniques: Because they do not consider the instantaneous pressures across the envelope, the previous models are completely unable to predict instantaneous infiltration. Realizing that weather is the dominant driving force for infiltration, researchers attempted, in a statistical sense, to fit the infiltration to the weather variables; that is, the infiltration was assumed to be linearly dependent on the temperature and wind speed:

$$Q = a + b\,\Delta T + c\,v \qquad (2)$$

where

Q	is the infiltration,
ΔT	is the inside-outside temperature difference,
v	is the wind speed and
a,b,c	are regression constants.

In order to use this model, a great deal of data (infiltration, temperatures, and wind speed) are taken at a particular site and the constants a,b,c are fit to it; once the constants have been found, the infiltration can be calculated from the weather variables using the above equation. Such regression equations have been found to be quite accurate for the site at which the data was taken;[2-4] however, if the same constants are tried at another site or if the weather variables are outside the range of the initial data, the results are completely unreliable. Furthermore, since the regression constants have no physical meaning, it is impossible to formulate a method that converts one set of regression constants for one particular site into those for another site.

Because only the weather variables appear specifically, the effect of envelope leakage is not evident. While it can be assumed that the leakier the structure, the more the infiltration, a linear regression fit does not predict how the infiltration of the structure will change if the leakage of the envelope is decreased.

- Detailed Models: Models are now being developed that perform very detailed calculations to find the instantaneous infiltration. Basically, this type of model calculates the pressure distribution everywhere (maintaining self-consistency) and from that pressure distribution it calculates the flow through each leak. This computation requires intimate knowledge of the location and

characteristics of each leak, (e.g., crack geometries and distribution, precise siting and terrain information, etc.) as well as the information necessary to calculate the pressure drops. While such detailed models can be made quite general and still be very accurate, they do require, however, that a large body of information about the structure be acquired.

In some detailed models[5] the pressure drop across the envelope is explicitly measured and combined with leakage characteristics of the envelope to find the infiltration. While this model can be very accurate in predicting infiltration, it does require constant monitoring of the pressures and, thus, it is clearly impractical for large-scale measurements.

Generally speaking, the large body of information required to determine infiltration makes these detailed models unsuitable for most applications. In a computer design program, it would be not only unreasonable but impossible for a designer or engineer to specify the location and size of every crack. For field testing, it would take an unreasonable length of time to locate and characterize each leak — assuming it were possible. Detailed techniques, then, are most suited to intensive research applications.

Clearly, none of these model types is adequate for predicting infiltration in the general case. What is needed is a simple, physical model of infiltration that allows infiltration to be calculated from a few easily measurable quantities and does not need to be modified for different climates or structure types.

This report introduces an infiltration model that sacrifices accuracy for versatility and simplicity. Rather than predicting accurately the weather-induced infiltration of a particular structure, the model is designed to calculate the infiltration of a general structure. Furthermore, the model predicts the impact of retrofits or other changes in the building envelope on the basis of performance changes effected in a few measurable parameters:

1) The leakage area(s) of the structure.
   The leakage area is the parameter that describes the tightness of the structure (obtained by pressurization). Most retrofits will affect the leakage area or the leakage distribution.

2) The geometry of the structure.
   The height and other geometric quantities are usually known or can be directly measured.

3) The inside-outside temperature difference.
   The temperature difference gives the magnitude of the stack effect. It is also necessary for calculating the energy load due to infiltration.

4) The terrain class of the structure.
   The terrain class of the structure is determined by the density of other buildings and obstructions that influence the dependence of wind speed on height near the structure. Knowing the terrain class of the structure allows the use of off-site weather data for calculating wind-induced pressures.

5) The wind speed.
   The wind speed is required to calculate the wind-induced infiltration for comparison with the stack effect.

Using standard wind formulae (see Table I.1) the wind speed used by the model can be calculated from a wind speed measured on any weather tower in the area. Thus, on-site weather collection is not necessary. The only requirement is that the measured wind data is for the "same wind", i.e., there can be no mountains or other major disturbances in terrain between the site and the wind tower.

THEORY

For this model, we assume that the structure is a single, well-mixed zone; we use typical shielding values for a simple rectangular structure and neglect terms that depend on the sign of the temperature difference. Most importantly, we split the problem into two distinct parts: the wind-regime, where the dynamic wind pressure dominates the infiltration, and the stack regime, where the temperature difference dominates the infiltration. Infiltration in the two regimes is expressed as follows:

$$Q_{wind} = f_w^* A_o v' \tag{3.1}$$

$$Q_{stack} = f_s^* A_o \sqrt{\Delta T} \tag{3.2}$$

where

A_o is the total leakage area of the structure [m^2],

Q_{wind} is the infiltration in the wind-regime [m^3/sec],

Q_{stack} is the infiltration in the stack regime [m^3/sec],

f_s^* is the reduced stack parameter [m/s/$\sqrt{K}$],

f_w^* is the reduced wind parameter,

v' is the (weather tower) wind speed [m/sec] and

ΔT is the inside-outside temperature difference [^oK].

Derivations for reduced parameters and a complete delineation of the assumptions are given in Appendix I and the results are given below.

The reduced wind parameter is given by the following expression:

$$f_w^* = C' \left[(1 - R)^{1/3} \right] \left[\frac{\alpha \left[\frac{H}{10}\right]^{\gamma}}{\alpha' \left[\frac{H'}{10}\right]^{\gamma'}} \right] \qquad (4)$$

where

C' is the generalized shielding coefficient,

R is the vertical leakage fraction
(i.e., the fraction of leakage in the floor and ceiling)

α, γ are terrain parameters

H is height of the structure [m] and

H' is the height of the wind measurement [m].

The reduced wind parameter contains three terms: the generalized shielding parameter, the R factor, and the terrain factor. The first term describes the shielding around the structure; we have used wind tunnel data[6] to find the generalized shielding coefficient for the case where there are no significant obstructions in the vicinity of the structure and have broadened the concept to allow for five different classes of shielding. Shielding class I is the unobstructed case and the values of the other classes reflect the fact that increasing the amount of obstructions near the structure will lower the pressures acting on that structure. Although shielding values in each class are

potentially measurable quantities, lacking direct experimental evidence, we have simply used equally-spaced (pressure) intervals as the separation between classes and have used suitably qualitative descriptions to define them. Work remains to be done to give these shielding classes proper experimental corroboration.

The second term in the reduced wind parameter expression accounts for the fact that the amount of leakage area available to the wind is reduced as the leakage area is shifted from the walls to the floor and ceiling. That is, for a given total leakage area, as R is increased there is less leakage area exposed on the walls; thus, since there is no direct wind effect on the floor and ceiling (due to our assumption of good shielding) the amount of air flow due to wind must decrease. Furthermore, in the limit of R=1 there will be no infiltration due to the wind.

The third term in the reduced wind parameter expression accounts for the fact that the wind measured on a weather tower will not be the same as the effective wind speed at the structure. To compensate for this effect we use standard wind engineering formulae[7] to translate the wind in one terrain and at one height to the same wind in another terrain and at another height. The primed quantities in the reduced wind parameter expression refer to the variables at the wind-measurement site, and the unprimed ones refer to the variables at the structure.

At first sight, terrain and shielding appear to be the same thing; the difference, however, is that of scale. Shielding refers to wind obstructions within a few typical dimensions of the structure and is, therefore, a local manifestation. Terrain effects refer to the general roughness of the surrounding countryside and are, therefore, global effects. (Tables containing the shielding and terrain parameters for different classes can be found at the end of Appendix I.)

The reduced stack parameter is given by the following expression:

$$f_s^* = \frac{(1 + R/2)}{3} \left[\frac{\sqrt{8\,\beta^o}\ \sqrt{1 - \beta^o}}{\sqrt{\beta^o} + \sqrt{1 - \beta^o}} \right] \sqrt{\frac{gH}{T}} \qquad (5)$$

where

g is the acceleration of gravity [9.8 m/s^2],

H is height of the structure [m],

T is the inside temperature [295K] and

f_s is the (dimensionless) stack parameter.

β^o is the (dimensionless) height of the neutral level.

The neutral level, β^o, is the height above the floor divided by the height from floor to ceiling at which the pressure inside exactly equals the pressure outside (due to the stack effect). Although this variable is experimentally determinable,[8] it is quite difficult to conduct this experiment. A byproduct of the calculation that leads to the stack equation above is a relation between the neutral level and the difference in the ceiling/floor leakage:

$$X = \frac{\frac{4}{3}(1-R)\left[(\beta^o)^{3/2} - (1-\beta^o)^{3/2}\right] + R\left[\sqrt{\beta^o} - \sqrt{1-\beta^o}\right]}{\sqrt{\beta^o} + \sqrt{1-\beta^o}} \qquad (6)$$

where

$X = \frac{A_{ceiling} - A_{floor}}{A_o}$ is the ceiling-floor leakage difference.

Unfortunately, this equation gives X in terms of β^o rather than the other way around. Numerical means, however, can be used estimate the value of the neutral level for a given value of X. Rather than requiring this laborious step each time, we have developed an approximation formula from this determining equation for the reduced stack parameter:

$$f_s^* = \frac{(1 + R/2)}{3}\left[1 - \frac{X^2}{(2-R)^2}\right]^{3/2}\sqrt{\frac{gH}{T}} \qquad (7)$$

This formula is correct up to the fourth order in X and has the correct limit as X approaches unity.

Superposition Law for Infiltration

We now have expressions that allow us to calculate the stack-induced infiltration and the wind-induced infiltration; the only problem that remains is that of combining them. In general, the interaction of such independent phenomena will be quite complicated but, in our simplified approach, we look only at the way in which each affects the differential pressure. Since both the stack effect and the wind effect influence the pressure distribution, we assume that their superposition can be treated by simply adding their pressure effects. Based on our assumption, a

square-root of dependence of flow-on pressure, it is reasonable to assume that stack-induced and wind-induced infiltration add in quadrature.

$$Q = \sqrt{Q_{stack}^2 + Q_{wind}^2} \tag{8}$$

where

Q is the combined infiltration [m^3/s]

In a previous work[13] the authors demonstrated that whenever the wind effect or stack effect dominates, the first-order cross term vanishes, making this type of combinatorial rule possible (i.e., there is no term of the form $Q_{stack} \times Q_{wind}$ in the above expression). Accurate prediction of the infiltration in the intermediate region requires detailed knowledge of both the weather and the structural parameters; hence, our simple model will be the least accurate in the region where the wind and stack infiltrations are equal.

RESULTS

Fifteen different sites were selected from the literature to represent wide variability in climate, house construction, and measured infiltration rates.[9-11] In all cases, leakage data obtained by fan pressurization was available, permitting us to calculate the leakage area. (Note that in Fig. 1. the leakage area varies by a factor of 16 from tightest to loosest.) The terrain class and the fraction of leakage in the floor and ceiling were estimated from the qualitative description of each site.

Appendix II contains tables providing data for each of the 15 sites; also included is the method of calculating leakage area. Figure 1 presents a bar graph showing the leakage area of each site. For most of the sites, the data consists of several short-term infiltration measurements made on a single day. Most infiltration measurements were made using a tracer gas decay technique[4] which measured infiltration over a one-hour period with 5%-10% accuracy. For each measured infiltration point, a predicted infiltration was calculated from the weather variables and house parameters. Figures 2 and 3 contain the plots of predicted vs measured infiltration. Figure 4 displays the deviation of the predicted infiltration (by the percentage difference from the measurement) vs. the leakage area (cm^2) for that site.

DISCUSSION

Considering the simplicity of the model and the fact that there are no adjustable parameters,* the agreement is good. However, there are a few sites that do not show particularly good agreement: some overpredict and some underpredict. In order to explain these discrepancies, we examined other factors that may affect the infiltration.

The biggest single factor affecting the accuracy of our model is the assumption that directional effects are unimportant. Directional effects could become important if the leakage of the walls varies from wall to wall, or if the shielding varies from face to face — either of which is possible. Directional effects could be especially important for the data contained herein because all of the weather and infiltration data were short-term — decreasing the likelihood that the wind direction was random.

Aside from the directional dependence, nonuniformity of wall leakage area will cause a relative decrease in the actual wind-induced infiltration. For example, if one wall of a structure is much leakier than the rest, it will act like a wind trap: when the wind blows on that wall, the internal pressure will rise to mitigate the air flow through that face. Thus the wind-driven infiltration ought to be lower for nonuniform leakage than for uniform leakage. Even though we have not demonstrated it in our derivation, it is generally true that (on average) any directional effects will lower the infiltration (i.e., for some directions the infiltration may be increased by nonuniform leakage but, if wind direction is averaged, the infiltration will be lowered).

Most likely, shielding will be the least uniform when it is the greatest, suggesting that directional effects should be more pronounced in more highly shielded situations. If we look at all of the shielding class 5 structures (sites 2,8,13) we see a definite pattern of overprediction (19%,43%,19% respectively). While in no way conclusive, this may indicate that directional effects are significant for these structures.

---

* We use "adjustable" to imply that there is no physical meaning associated with that parameter (e.g., regression coefficients). While physical parameters (e.g., R) may be estimated, they are not adjusted to improve the fit.

Our model has also assumed that the floor and ceiling are unaffected by the wind. This assumption is violated whenever a leak through the floor or ceiling leads directly into the wind stream, such as occurs with a vent, chimney or flue. If the wind is blowing over the top of a flue, the infiltration will be greatly increased over what it would be otherwise. However, this effect is very directionally dependent because of the turbulence caused by the wind interacting with the roof structure. The effect will be largest when the flue has a large leakage area; thus we expect to see a large effect in structures that have undampered fireplace chimneys. Two of the test structures had undampered chimneys (10,14) and both showed significant underprediction (-16%, -22% respectively).

While the accuracy of the model is sufficient for a wide variety of applications, the shortcomings described above suggest ways in which accuracy can be improved. Not only can we include new parameters to account for local shielding, but we can extend the model to account for stack flows through vents and flues and for active systems (e.g., furnace fans), all of which may interact with natural ventilation.

Graphical Method

Some of the direct calculations (especially of the stack parameter) are difficult to do on a hand calculator in the field. We, therefore, have developed a graphical method of obtaining the neutral level, the stack parameter, and the infiltration from the data. Aside from the ease of operation, the graphical approach allows one to see the effects of different quantities directly — in a far clearer way than the bare equations provide.

Figure 4 presents a graph of the stack parameter (which is the reduced stack parameter without the $\sqrt{gH/T}$ term) vs the neutral level for several different values of the vertical leakage fraction, R. Note that the solid portion of each curve represents the physically allowed region; that is, for a given value of R, the neutral level can have only a limited range of values — it is for the case of R=1 alone that the neutral level can take on its full range from 0 to 1.

The neutral level is not the parameter that is usually measured, however; it is the ceiling-floor leakage difference, X, that is most often known. Accordingly, Figure 6 contains a plot of X versus neutral level, again for several values of R. These two curves can be parametrically combined to eliminate the neutral level yielding the relationship

between the stack parameter and the ceiling-floor leakage difference; Figure 7 shows this function.

The fact that the reduced parameters do not depend on weather variables implies that there are just two (simple) degrees of freedom in the infiltration expression; that is, the only two variables that are time dependent in the superposition of infiltration are the wind and the temperature difference. Thus, we can use a graph of the wind vs temperature difference to find the total infiltration. Figure 8 is such a graph and the following paragraph describes how it is used.

Having found the stack parameter, we can find the reduced stack parameter by multiplying by $\sqrt{gH/T}$. From the terrain parameters and the shielding class, we can find the reduced wind parameter as well. These parameters are then combined with the weather variables (temperature difference and measured wind speed) to find a point on the graph. This point corresponds to a particular ratio of infiltration to total leakage area, as can be read from the curved lines of Figure 8. Finally, the ratio is multiplied by the total leakage area to find the infiltration. Since only the weather variables change over time, this method can be used repeatedly on a single site with a minimum of calculation.

FUTURE DIRECTIONS

The discussion of results indicated several areas in which the model might be improved. Furthermore, some effects influencing certain structures might not have been apparent in our 15 sites -- for example, directional effects and unevenly distributed leakage, multichamber effects, vents, occupancy effects and linear leakage. Accordingly, we will attempt to address some of these issues here.

Directional Effects

If, within a given period of observation, the wind direction is suitably random, the orientation of the building or unevenly distributed leakage will not affect infiltration. If, however, the wind comes from a restricted range of directions, the orientation of the structure and its leakage distribution can affect the infiltration. Similarly, directional differences in shielding will cause the infiltration to be directionally dependent. Conceptually, this situation can be handled by adding an additional factor to the reduced wind parameter; this factor would be a function of the wind direction and would contain information regarding the leakage distribution from wall to wall, as well as the effects of localized shielding. Furthermore, to preserve the current

formalism, the angle average of this function would be unity. (Conceivably, this function could be subsumed into the generalized shielding coefficient.) Little more can be said about directional effects until more data has been taken. Theoretical work remains to be done on the effect of localized leakage from wall to wall, and experimental work remains to be done on localized shielding of one wall as opposed to another.

Vents

In our analysis of infiltration we assumed that all of the significant air flow took place directly through the shell of the envelope; in most cases this is true, but in a large proportion of structures a substantial amount of air flows through vents a significant fraction of the time. We define a vent to be any pathway that leads from the inside of the structure to the outside (e.g., chimney, exhaust vent, etc.). Vents may be powered (by a fan or heat source) or unpowered; examples, of powered vents are furnace flues and exhaust vents with fans; unpowered vents would be chimneys or flues with no heat sources, or exhaust vents with no fan in operation.

Since powered vents have their own pressure source that is causing air flow, it is clear that they must be treated separately from the rest of the infiltration. Less obvious is the fact that unpowered vents must also be treated separately because vents generally "see" a different pressure across them than does the part of the envelope they pierce. For example, most flues and exhaust vents go through the ceiling of the structure and stick out above the roof; they are specifically designed to protrude into the free-stream wind and, hence, will experience a very different pressure from that of a (well-shielded) ceiling. (An unpowered vent that does not protrude away from the envelope (e.g., dryer vent) can be considered as a hole not a vent and thus treated in the standard model.

The flow through these vents is calculated by ignoring the presence of the wind and stack infiltrations and treating each vent independently. If the vent is powered by a fan, we can assume that the flow through the vent will simply be the fan rating. The problem becomes far more difficult if the vent is powered by a heat source (e.g., fireplace or furnace flue). Modera and Sherman[12] have derived a model of the flue flow using the leakage area of the flue, the leakage area of the structure, and the waste heat of the appliance. We derive the following

cubic equation for the flow up the flue:

$$\left[1+\frac{A_{vent}^2}{A_o^2}\right] Q_{vent}^3 + \left[2+\frac{A_{vent}^2}{A_o^2}\right] Q_o\, Q_{vent}^2 + Q_o^2\, Q_{vent} = 2A_{vent}^2\, gh'\, Q_o \qquad (9)$$

where

Q_{vent} is the flow rate up the vent [m^3/s],

h' is the stack height (above the neutral level)[m],

A_o is the leakage area of the house (excluding vent) [m^2] and

A_{vent} is the leakage area of the vent [m^2].

Q_o is a function of the waste heat that goes up the stack:

$$Q_o = \frac{\Phi}{\rho\, C_p\, T} \qquad (10)$$

where

C_p is the specific heat of air [1000 joules/kg-K] and

Φ is the waste heat [watts].

Because this expression ignores the effect of the outside weather on the stack flow, we must evaluate the weather-driven case as well. As suggested earlier, a possible method for combining these two flows would be in quadrature.

If the vent is unpowered, the driving force, as in the standard model, is the weather, but we cannot use the same expressions. In this case, the pressure across the vent can be given by the following expression:

$$\Delta P = \tfrac{1}{2}\, \rho\, v^2 + \rho g h' \frac{\Delta T}{T} \qquad (11)$$

where

v is the velocity at the top of the stack [m/s],

h' is the height of the stack (above the neutral level)[m],

which leads to an expression for the flow through the vent:

$$Q_{vent} = A_{vent}\, v \sqrt{\left| 1 + \frac{2gh'}{v^2}\frac{\Delta T}{T} \right|} \qquad (12)$$

Unlike the standard infiltration model, this (unpowered) vent flow model is dependent on the sign of the temperature difference; in the winter the effects of the stack and wind terms are in the same direction, but in the summer the stack and wind effects act oppositely and, if the wind in low enough and the outside temperature high enough, the flow in the stack will reverse.

Because the stack can be assumed to stick up into the free-stream wind, we can approximate the velocity by the velocity at roof height. The second term is strictly true only if it is warmer inside than out and if the stack can be assumed to be at indoor temperature. If the stack is at outside temperature, then h′ should be interpreted as the difference between the neutral level and the bottom of the stack. While this simplistic approach is physically valid, it has not as yet been validated.

Once the individual flows from each of the vents have been calculated, it remains to combine them with each other and the stack and wind infiltration to find the total infiltration. We must separate the vent flow into balanced and unbalanced flows; vent flow is balanced if there is vent flow of the opposite direction that compensates for it; that is, if there is an exhaust vent, it will be balanced only if there is an intake vent of the same air flow. Balanced flow does not affect the interior pressure as does unbalanced flow, which has no compensating airflow. Balanced flow will add simply to the total infiltration while unbalanced flow (like the stack and wind flows) will add in quadrature:

$$Q_{total} = Q_{balanced} + \sqrt{Q^2_{unbalanced} + Q^2_{wind} + Q^2_{stack}} \qquad (13)$$

The balanced and unbalanced flows can be expressed as follows:

$$Q_{balanced} = \mathrm{MIN}\left(\Sigma\, Q^{+}_{vent},\ \Sigma Q^{-}_{vent} \right) \qquad (14.1)$$

$$Q_{unbalanced} = \mathrm{MAX}\left(\Sigma\, Q^{+}_{vent},\ \Sigma Q^{-}_{vent} \right) - Q_{balanced} \qquad (14.2)$$

where

Q^{+}_{vent} is the vent infiltration [m^3/s] and

Q^{-}_{vent} is the vent exfiltration [m^3/s].

Generally speaking, vent infiltration will seldom be a factor, except when air-to-air heat exchangers are used. These heat exchangers run two streams of air -- one inside to out, the other outside to in -- and the heat from one is transferred to the other, supplying "preconditioned" fresh air to the structure. This process is a perfect example of balanced vent flow; the two air streams balance each other and increase infiltration without changing the internal pressure.

Very little work has been done on the effect of vents on the total infiltration. The simple model of vents presented here may be adequate for determining the total infiltration, but only experimental tests can validate it.

Occupancy Effects

Occupancy effects are one of the hardest problems to deal with in constructing an infiltration model. Most other problems can be modeled, albeit with simplified models, but occupancy effects require a socio-physiological model of human comfort and behavior, which we are unable to present. Certain general features of occupancy effects can be enumerated, however: Door openings and closings can be modeled as a discrete amount of flow; window openings can be treated as an increase in the wall leakage area and. if the windows are distributed on different sides of the structure, they can be handled by the standard model. Fortunately, occupancy effects matter the most when infiltration matters the least — that is, occupants are most likely to open windows when the outside temperature is in the comfort range. Hence, the need for modeling infiltration at these times is minimal.

Multichamber Effects

In a large structure like an office building or an apartment building, the assumption of a single well-mixed interior zone breaks down. In this case it is not sufficient to calculate the total amount of outside air that infiltrates the structure; what is important is to be able to calculate how much fresh air gets into each chamber individually, and even how much air is exchanged between the chambers. In these

structures, then, a multichamber model is needed.

Much work remains to be done before an acceptable multi-chamber model can be developed. As yet, there exists no accurate method to measure the actual infiltration in the multichamber case, nor is there a method to measure the leakage between the chambers. Until these experimental problems have been solved, the existence of a multichamber model remains a moot point.

Linear Leakage

From the leakage measurements of the previous chapter, we concluded that leakage can be best described by its square-root dependence on pressure that leads to the definition of the leakage area. This assumption appears to be borne out reasonably well by the data collected in this section. In some situations, however, square-root leakage dependence is insufficient and leakage must be described by a linear model. Because such a drastic change in the leakage model would require a complete reworking of the infiltration model, no attempt has been made to apply it to any real situation. It remains to be seen whether such a model will ever be required, or whether the current infiltration model will be sufficient for all real cases.

APPENDIX I

CALCULATION OF ISOLATED INFILTRATION

Infiltration is caused by differential pressures across the envelope of a structure; these pressures are, in turn, caused by the action of the weather on the structure. Weather-induced pressures can be separated into two types: Stack Effect pressures are created by an indoor-outdoor temperature difference, and Wind Effect pressures are created by the dynamic forces exerted by the wind on a stationary object. In this Appendix we calculate the infiltration separately for each of these two effects.

The pressures induced by the stack and wind effects cause flow through the leakage sites in the building envelope. As discussed in the text, we use a leakage model that assumes the flow to be dominated by inertial effects, implying that an area can be defined to characterize the leakage:

$$Q_j = A_j\sqrt{\frac{2}{\rho}\Delta P_j} \qquad (I.1)$$

where

Q_j is the flow through the jth leakage site [m^3/s],

A_j is called the leakage area of the jth site [m^2],

ΔP_j is the pressure drop across the jth site [Pa] and

ρ is the mean density of air[1.2 kg/m^3].

Although every leakage site can be given a leakage area, in any real situation it will be practically impossible to measure all of the sites in the envelope individually. Hence, we will limit the number of leakage variables by considering each face of the structure (i.e., floor, walls, ceiling) to have a single leakage area. Furthermore, we will treat the stack and wind effects separately (i.e., without taking each other into account).

PART I — Stack Effect

The stack-effect pressure is caused by the existence of bodies of air whose differing temperatures cause differing densities. From the condition of hydrostatic equilibrium, we know that the change in pressure with respect to height is proportional to the density.

$$\frac{dP}{dh} = - \rho g \qquad (I.2)$$

where

P is the static pressure [Pa],

h is the height [m],

ρ is the density of that body of air [kg/m^3] and

g is the acceleration of gravity [9.8 m/s^2].

In the case of a structure, the inside and outside bodies of air will usually be of different temperatures: therefore, there will be a differential surface pressure that changes with height:

$$\frac{d\Delta P}{dh} = - \rho g \left(1 - \frac{\rho'}{\rho}\right) \qquad (I.3)$$

where

ΔP is the differential surface pressure [Pa].

ρ is the density of outside air [1.2 kg/m^3],

ρ' is the density of inside air [kg/m^3],.

Using the ideal gas law, we can replace the density difference factor with a temperature difference factor:

$$\frac{d\Delta P}{dh} = - \rho g \frac{\Delta T}{T} \qquad (I.4)$$

where

ΔT is the inside-outside temperature difference [K] and

T is the inside temperature [295K].

We can now integrate this expression to find the actual pressure difference:

$$\Delta P = \Delta P_o - \rho\ g\ h\ \frac{\Delta T}{T} \qquad (I.5)$$

where

ΔP_o is the constant of integration [Pa].

This constant of integration corresponds to an internal pressure shift; it will be fixed by the requirement that the volume of air entering the structure must be equal to the volume of air leaving it.

We now rewrite that expression,

$$\Delta P = P_s\ (\beta^o - \beta) \qquad (I.6)$$

where

P_s is the stack pressure [Pa],

β is the (dimensionless) height and

β^o is the (dimensionless) height of the neutral level.

In the above expression we have used the following definitions:

$$P_s = \rho\ g\ H\ \frac{\Delta T}{T} \qquad (I.7.1)$$

$$\beta = \frac{h}{H} \qquad (I.7.2)$$

$$\Delta P_o = P_s\ \beta^o \qquad (I.7.3)$$

where

the neutral level is the height at which the inside and outside static pressures are equal. H is the height of the structure [m] and (Note that we have substituted the height of the neutral level for the internal pressure shift as our unknown constant of integration.)

We now have an expression that relates the differential pressure to the stack pressure, the neutral level, and the position on the structure. In order to calculate the air flow through the envelope, we must integrate the differential pressures with the air leakage over the entire envelope, making sure to keep track of the infiltration and exfiltration separately.

We are assuming that the floor and ceiling are each at a single height and that their leakage can be considered uniform, thus eliminating the need for integration to calculate the flow through these surfaces. Rewriting the expressions by using the definition that the floor is at $\beta=0$ and, therefore, the ceiling is at $\beta=H$, we get:

$$Q^{-}_{ceiling} = A_c \sqrt{\frac{2}{\rho} P_s (\beta^o - 1)} \qquad (I.8.1)$$

$$Q^{+}_{floor} = A_f \sqrt{\frac{2}{\rho} P_s (\beta^o)} \qquad (I.8.2)$$

$$Q^{+}_{ceiling} = Q^{-}_{floor} = 0 \qquad (I.8.3)$$

where

A_c is the leakage area of the ceiling[m^2] and

A_f is the leakage area of the floor[m^2].

The superscripts +/- imply infiltration/exfiltration, respectively.

In stack-dominated flow there is no infiltration through the ceiling nor is there any exfiltration through the floor because of the sign of the pressure difference across them.

We can find the infiltration through the walls by integrating from the floor to the neutral level, and the exfiltration by integrating from the neutral level to the ceiling:

$$Q^{+}_{w} = A_w \sqrt{\frac{2}{\rho} P_s} \int_0^{\beta^o} \sqrt{\beta^o - \beta}\, d\beta \qquad (I.9.1)$$

$$Q^{-}_{w} = A_w \sqrt{\frac{2}{\rho} P_s} \int_{\beta^o}^{1} \sqrt{\beta - \beta^o}\, d\beta \qquad (I.9.2)$$

where

Q_w is the infiltration/exfiltration through a wall [m^3/s],

A_w is the leakage area of the walls [m^2].

If we now make the useful definitions.

$$A_o = A_w + A_c + A_f \qquad (I.10.1)$$

$$R = \frac{A_c + A_f}{A_o} \qquad (I.10.2)$$

$$X = \frac{A_c - A_f}{A_o} \qquad (I.10.3)$$

where

A_o is the total leakage area [m^2].

R is the fraction of leakage in the floor and ceiling and

X is the leakage distribution parameter.

we can rewrite the expressions for the total stack infiltration and exfiltration:

$$Q^{+}_{stack} = A_o \sqrt{2gh\frac{\Delta T}{T}} \left[\frac{R - X}{2} \sqrt{\beta^o} + \frac{2}{3} (1 - R) (\beta^o)^{3/2} \right] \qquad (I.11.1)$$

$$Q^{-}_{stack} = A_o \sqrt{2gh\frac{\Delta T}{T}} \left[\frac{R + X}{2} \sqrt{1 - \beta^o} + \frac{2}{3} (1 - R) (1 - \beta^o)^{3/2} \right] \qquad (I\ 11.2)$$

Treating air as an incompressible gas requires that the infiltration and exfiltration be equal. Therefore, the relationship between the neutral level (β^o) and the vertical leakage distribution parameter (X) is fixed:

$$X = \frac{\frac{4}{3}(1-R) \left[(\beta^o)^{3/2} - (1-\beta^o)^{3/2} \right] + R \left[\sqrt{\beta^o} - \sqrt{1-\beta^o} - \right]}{\sqrt{\beta^o} + \sqrt{1 - \beta^o}} \qquad (I.12)$$

Using this expression, any one of the parameters from the set

$\{\beta^o, X, R\}$ can be found from the other two.

Because the expressions for infiltration and exfiltration are equal, it does not matter what linear combination we use to find the actual air flow; for ease of calculation and minimization of errors, we use the average of the two expressions:

$$Q_{stack} = \frac{A_o}{3}\sqrt{2gh\frac{\Delta T}{T}}\,(R+2)\,\frac{\sqrt{\beta^o}\,\sqrt{1-\beta^o}}{\sqrt{\beta^o}+\sqrt{1-\beta^o}} \qquad (I.13)$$

While it is possible to measure the neutral level directly[8], in most cases it will be the variable X that will be available. Accordingly, we have used approximation methods to find an expression for the infiltration that contains X instead of the neutral level:

$$Q_{stack} = \frac{A_o\sqrt{gh\frac{\Delta T}{T}}}{3}\,(1+R/2)\left[1-\frac{X^2}{(2-R)^2}\right]^{3/2} \qquad (I.14)$$

Summary

In this part of the Appendix we have derived formulae for calculating infiltration due to the presence of an indoor-outdoor temperature difference. Below is a listing of these equations with some definitions of terms.

$$Q_{stack} = A_o\, f_s^*\,\sqrt{\Delta T} \qquad (I.15.1)$$

$$Q_{stack} = A_o\, f_s\sqrt{gH\frac{\Delta T}{T}} \qquad (I.15.2)$$

where

f_s^* is the reduced stack parameter [m/s/$\sqrt{K}$] and

f_s is the (dimensionless) stack parameter.

As is obvious from these two equations,

$$f_s^* = f_s \sqrt{\frac{gH}{T}} \qquad (I.16)$$

The stack parameter has two different expressions that are essentially equal: the exact expression which requires knowledge of the height of the neutral level,

$$f_s = \frac{(1 + R/2)}{3} \left[\frac{\sqrt{8}\sqrt{\beta^o}\sqrt{1 - \beta^o}}{\sqrt{\beta^o} + \sqrt{1 - \beta^o}} \right] \qquad (I.17.1)$$

and the approximate expression which requires knowledge only of the relative leakiness of the floor and the ceiling.

$$f_s = \frac{(1 + R/2)}{3} \left[1 - \frac{X^2}{(2 - R)^2} \right]^{3/2} \qquad (I.17.2)$$

Note that X=0 implies $\beta^o = 1/2$ which implies that both terms in brackets are equal to unity. Furthermore, there is an exact relationship between X and β^o as given previously.

PART II — Wind Effect

The wind pressure is caused by the loss of kinetic energy associated with the deceleration of wind when it strikes a fixed object. This relation is given by the expression,

$$\frac{dP}{dv} = -\rho v \qquad (I.18)$$

where

P is the static pressure [Pa] and

v is the real free-stream wind speed [m/s].

Care must be taken in determining velocity in the above expression. There are two factors which complicate the measurement of the free-stream wind speed· terrain and shielding.

Terrain effects result from the fact that the measurement of wind speed may not occur at the same height or in the same general geographic terrain as the infiltration measurements (i.e., both the height and the geography can affect the free-stream wind speed). Conventionally, we define the wind speed, v, to be the free-stream wind speed at the

ceiling height of the structure. This convention for defining wind speed necessitates a method for converting wind speed obtained from a weather-tower measurement to a local free-stream wind speed. To do this, we make use of standard wind-engineering formulae[7]:

$$v = v_o \alpha \left[\frac{H}{10}\right]^{\gamma} \tag{I.19}$$

where

v is the actual wind speed

v_o is the wind speed at standard conditions

α, γ are constants that depend on terrain class

To calculate the wind speed at one site from measured data at another site, we first use the above formula to calculate the standard wind speed for the measurement site; then the standard wind speed is used to calculate the wind speed at the desired site. Standard conditions are defined to be a height of 10 m and a terrain of class II. The following formulae are useful in calculating the actual wind speed:

$$v = v_o \alpha \left[\frac{H}{10}\right]^{\gamma} \tag{I.20.1}$$

$$v' = v_o \alpha' \left[\frac{H'}{10}\right]^{\gamma'} \tag{I.20.2}$$

$$v = v' \left[\frac{\alpha \left[\frac{H}{10}\right]^{\gamma}}{\alpha' \left[\frac{H'}{10}\right]^{\gamma'}}\right] \tag{I.20.3}$$

In these expressions, the primed quantities are from a wind measurement site. Values for the two parameters dependent on terrain class are shown in Table I.1.

From the above expression, we can define a terrain factor, f_T, that converts measured wind speed into effective wind speed:

$$f_T = \left[\frac{\alpha \left[\frac{H}{10}\right]^{\gamma}}{\alpha' \left[\frac{H'}{10}\right]^{\gamma'}}\right] \tag{I.21}$$

Although we can now calculate the free-stream wind speed, we are not yet able to calculate the wind pressures felt by the structure because we have not taken into account local shielding. Buildings and other obstructions within a few house-heights of the site will tend to slow or otherwise block the wind from having its full impact on the structure. To account for this phenomenon, we use a set of shielding coefficients* to convert the free-stream wind pressure into that actually felt by the structure. Thus,

$$\frac{dP}{dv} = - C \rho v \qquad (I.22)$$

where

C is the shielding coefficient.

In the general case, the shielding coefficient will be a function of incident wind angle and position on the surface of the structure; however, full-scale studies [13] have shown that the pressure distribution on flat faces can be adequately described by using the average pressure on the face.there is one (angle-dependent) shielding coefficient for each face of the structure.†

$$\frac{dP_j}{dv} = C_j \rho v \qquad (I\ 23)$$

where

P_j is the static pressure on the jth face [Pa]

C_j is the shielding coefficient for the jth face

---

* The term shielding coefficient is equivalent to the more standard term of exterior pressure coefficient; the only difference lies in the interpretation. We use the term shielding coefficient to mean the ratio of the average exterior wind pressure to the stagnation pressure at the ceiling height.

† The shielding coefficients are functionally dependent on the angle between the incident wind and the orientation of the structure. Since we will eventually average the shielding coefficients over angle, we have suppressed their explicit dependence on angle.

Integrating this equation yields,

$$P_j = P^j + C_j \ 1/2 \ \rho \ v^2 \qquad (I.24)$$

where

P^j is the jth constant of integration [Pa].

Leakage through the envelope allows the internal pressure to be affected by the wind; thus, there will be an internal shielding coefficient analogous to the external ones above:

$$P_o = P^o + C_o \ 1/2 \ \rho \ v^2 \qquad (I.25)$$

where

P^o is the interior constant of integration [Pa] and

C_o is the internal shielding coefficient.

Note that the internal shielding coefficient is not an independent quantity; like the neutral level in the stack-effect case, it is fixed by the equality of infiltration and exfiltration.

Since at zero wind speed the pressure across the envelope is zero, all of the integration constants must be equal; that is.

$$P^j = P^o \qquad \text{for all } j \qquad (I.26)$$

Furthermore, if we construct the differential surface pressure across the structure, the constant of integration will disappear altogether:

$$\Delta P_j = P_j - P_o \qquad (I.27.1)$$

$$= (C_j - C_o) \ 1/2 \ \rho \ v^2 \qquad (I.27.2)$$

To find the infiltration. we use these equations with the leakage function (Eq A.1):

$$Q^+_{wind} = v \sum_j A_j \sqrt{C_j - C_o} \qquad \text{for } C_j > C_o \qquad (I.28.1)$$

$$Q^{-}_{wind} = v \sum_j A_j \sqrt{C_o - C_j} \qquad \text{for } C_j < C_o \qquad (I.28.2)$$

where

Q^{+}_{wind} is the infiltration due to the wind [m^3/s] and

Q^{-}_{wind} is the exfiltration due to the wind [m^3/s].

Conceptually, we can solve the problem in the same way as in the stack-effect case: equate the infiltration and exfiltration to find C_o and then take the average of the infiltration and exfiltration to find the air flow. While the latter can be done, i.e.,

$$Q_{wind} = \frac{v}{2} \sum_j A_j \sqrt{\left| C_j - C_o \right|} \qquad (I.29)$$

the former cannot. The internal shielding coefficient, which is a function of the other shielding coefficients and leakage areas, cannot be found in general but rather, must be calculated numerically for specific values of the leakage areas and shielding coefficients.

Rather than accept the situation and require detailed knowledge about shielding and leakage, we shall make some physically reasonable assumptions and use approximation techniques to get a general solution. In most cases the ceiling and floor of a structure are well shielded (i.e., there is usually an attic, basement, or slab that protects these horizontal surfaces from direct wind effects). Accordingly, we assume that their shielding coefficients are negligible. In general, directional effects are not interesting; therefore, we average over incident wind angle, yielding,

$$Q_{wind} = \frac{A_o}{2} v \left[(1 - R) \left\langle \sqrt{\left| C_j - C_o \right|} \right\rangle + R \left\langle \sqrt{\left| C_o \right|} \right\rangle \right] \qquad (I.30)$$

where

$\langle \ldots \rangle$ indicates an average over direction

We have reduced the problem to the evaluation of average shielding coefficients, which are independent of the leakage areas. We must now evaluate the shielding coefficients to finish the calculation of the wind effect. In most cases, the shielding coefficients of a structure will not be known; therefore, we propose to use wind tunnel data for a typically shaped structure within a turbulent boundary layer. Such a

study was done at Colorado State University by Akins, et. al.[6]

It would be far more convenient to have an algebraic expression in closed form that describes the wind effect; accordingly, we have used the wind tunnel data to numerically fit these expressions to a functional form that describes the data to within 5%:

$$Q_{wind} = A_o \, v \, (1 - R)^{1/3} \, C' \qquad (I.31)$$

where

C' is the generalized shielding coefficient.

The aforementioned study considered only the case of the "self-shielded" structure. In any real situation, however, there will be local obstructions in the neighborhood of the building: we, therefore, propose to break the shielding into five classes, where class I is the "self-shielded" case and the remaining classes scale down the value of the shielding coefficients equally. Because we are assuming that all of the shielding coefficients scale the same way, C' but not n will be affected by a change in shielding class. Table I.2 contains the values of the generalized shielding coefficient C' for all five shielding classes.

We are now in a position to define the reduced wind parameter in a manner similar to that used for the reduced stack parameter; i.e.,

$$Q_{wind} = f_w^* \, A_o \, v' \qquad (I.32)$$

where

f_w^* is the reduced wind parameter:

$$f_w^* = C' \, (1 - R)^{1/3} \left[\frac{\alpha \left[\frac{H}{10} \right]^{\gamma}}{\alpha' \left[\frac{H'}{10} \right]^{\gamma'}} \right] \qquad (I.33)$$

Summary

In this part of the Appendix we have derived formulae for calculating infiltration due to the presence of steady-state wind impinging on the surface of the building, and we are now in a position to summarize the results. Below is a listing of these equations with some convenient definitions of terms.

$$Q_{wind} = A_o \, f_w^* \, v' \qquad (I.34.1)$$

$$Q_{wind} = A_o \, f_w \, v \qquad (I.34.2)$$

where

f_w^* is the reduced wind parameter and

f_w is the wind parameter.

These two parameters are related by the terrain factor:

$$f_w^* = f_w \, f_T \qquad (I.35)$$

The wind parameter is an approximate quantity that contains information about the general shielding and the leakage distribution:

$$f_w = C' \, (\, 1 - R \,)^{1/3} \qquad (I.36)$$

The quantities necessary for calculating the terrain factor and the generalized shielding coefficient are in tables at the end of this Appendix.

Table I.1. Terrain parameters for standard terrain classes

Class	γ	α	Description
I	0.10	1.30	Ocean or other body of water with at least 5 km of unrestricted expanse
II	0.15	1.00	Flat terrain with some isolated obstacles (e.g. buildings or trees well separated from each other
III	0.20	0.85	Rural areas with low buildings. trees, etc.
IV	0.25	0.67	Urban, industrial or forest areas
V	0.35	0.47	Center of large city (e.g., Manhattan)

Table I.2. Generalized shielding coefficient vs. local shielding

Shielding Class	C′	Description
I	0.324	No obstructions or local shielding whatsoever
II	0.285	Light local shielding with few obstructions
III	0.240	Moderate local shielding, some obstructions within two house heights
IV	0.185	Heavy shielding, obstructions around most of perimeter
V	0.102	Very heavy shielding, large obstruction surrounding perimeter within two house heights

APPENDIX II

DATA TABLES

This Appendix contains tables of data from 15 different sites around the country. Physical descriptions, geometric data, and measured leakage area are all displayed, as are the predicted and measured infiltrations for each site.

All data was extracted from the literature;[14-17] there are 15 sites taken from these three sources all of which were measured before the model was developed. The data extracted from reference 2 was collected by the authors.

Terrain Factor

The terrain factor displayed in these tables contains the terrain parameters and heights from both the wind measurement site and the test site. Specifically,

$$f_T = \frac{\alpha\left[\frac{H}{10}\right]^{\gamma}}{\alpha'\left[\frac{H'}{10}\right]^{\gamma'}}$$

where

f_T is the terrain factor,

H is the height [m] and

α, γ are the terrain parameters.

The terrain parameters can be found in Table I.1 of Appendix I. The primed quantities refer to the wind measurement site and the unprimed quantities refer to the test site.

Leakage Area

Generally, the leakage data extracted from the literature was not presented as "leakage area". In some cases, the leakage curves (for pressurization and depressurization) were given; in others only the flow rate at a specified pressure was provided. We had to devise a methodology for taking this type of data and converting it to leakage area for each case:

Low-Pressure Leakage Data. If leakage data was provided down to our reference pressure of 4 Pa , we can use the leakage model (i.e.

$$Q = A \sqrt{\frac{2}{\rho} \Delta P} \qquad \text{(II.1)}$$

where

Q is the air flow rate [m^3/s],

A is the leakage area [m^2] and

ΔP is the pressure drop [Pa])

to find the leakage area at the reference pressure:

$$A = Q(\Delta P_r) \sqrt{\frac{\rho}{2 \Delta P_r}} \qquad \text{(II.2)}$$

where

ΔP_r is the reference pressure [4 Pa] and

$Q(\Delta P_r)$ is the air flow at the reference pressure[m^3/s].

High Pressure Leakage Data. If only high-pressure leakage data is provided (i.e. the leakage curve was measured but not down to the reference pressure), we use an empirical formula to extrapolate the data down to the reference pressure. The leakage data is fit to a power law function of the form,

$$Q = C \left[\Delta P \right]^n \qquad \text{(II.3)}$$

where

C,n are found through linear regression.

After finding the two unknown parameters, we extrapolate down to find the flow at the reference pressure and use that in the previous formula to find the leakage area. Putting this equation in a form similar to the one used for low pressure leakage yields equations of the following form:

$$A = Q(\Delta P) \left[\frac{\Delta P_r}{\Delta P}\right]^n \sqrt{\frac{\rho}{2\,\Delta P_r}} \qquad \text{(II.4.1)}$$

or

$$A = C \left[\Delta P_r\right]^n \sqrt{\frac{\rho}{2\,\Delta P_r}} \qquad \text{(II.4.2)}$$

Note that all dependence on the reference pressure disappears for the special case of n=1/2.

Flow at Specified Pressure. If the only leakage data available is the leakage at a specified pressure, we cannot fit the data to any functional form. Some data[3] suggests that for a wide variety of envelope types the exponent in the above equation is 0.65. Accordingly, we will substitute 0.65 for n in the above expression and use the stated air flow and pressure to find C and, as in the previous case, the leakage area.

Infiltration Measurements

All of the infiltration measurements in this data were short-term tracer measurements using the decay technique. No attempt was made to quantify the effective volume of any of the test spaces; therefore, the physical volume was used to convert from air change rate to the infiltration.

In most cases, mixing problems were minimized by making sure that the tracer gas was well mixed before the decays had begun. This was done, whenever possible, by using the fan and duct system of the house; in lieu of that, additional mixing was supplied (e.g., mixing fans). Once the gas was well mixed, the additional mixing was stopped to prevent it from affecting the infiltration.

The error for this type of tracer gas measurement is typically about 10%.

Table 1 · Test results for test site #1

Site ID:	IVANHOE
Reference No.	2
House Volume[a]	480
No. of Stories	2
Leakage Area[b]	100
Floor Area[a]	174
Terrain factor	0.85
Shielding Class	3
Reduced wind parameter:	0.19
Reduced stack parameter[c]:	0.16
Description:	energy-efficient basement active solar sealed combustion wood stove vapor barrier

Predicted and Measured Infiltration[d]				
Stack	Wind	Total Predicted	Measured	Difference
27	27	38	58	-34%
27	55	61	58	5%
27	41	49	48	2%

---

1) SI units

2) cm^2

3) $m/s/K^{1/2}$

4) m^3/hr

Table 2 : Test results for test site #2

Site ID:	NOGAL
Reference No.	2
House Volume[a]	290
No. of Stories	1
Leakage Area[b]	960
Floor Area[a]	107
Terrain factor	0.70
Shielding Class	5
Reduced wind parameter:	0.08
Reduced stack parameter[c]:	0.10
Description:	energy-efficient slab on grade active solar and forced air vapor barrier

Predicted and Measured Infiltration[d]				
Stack	Wind	Total Predicted	Measured	Difference
60	47	76	64	19%

1) SI units

2) cm^2

3) $m/s/K^{1/2}$

4) m^3/hr

Table 3 : Test results for test site #3

Site ID:	TELEMARK
Reference No.	2
House Volume[a]	480
No. of Stories	2
Leakage Area[b]	140
Floor Area[a]	197
Terrain factor	0.85
Shielding Class	2
Reduced wind parameter:	0.22
Reduced stack parameter[c]:	0.12
Description:	energy-efficient basement radiant oil fired heat — solar hot water vapor barrier seal combustion wood stove

Predicted and Measured Infiltration[d]				
Stack	Wind	Total Predicted	Measured	Difference
31	53	61	63	-3%
30	42	52	48	8%
30	32	44	38	16%

1) SI units

2) cm^2

3) $m/s/K^{1/2}$

4) m^3/hr

Table 4 : Test results for test site #4

Site ID:	TOREY PINES
Reference No.	3
House Volume[a]	233
No. of Stories	3
Leakage Area[b]	200
Floor Area[a]	220
Terrain factor	0.90
Shielding Class	4
Reduced wind parameter:	0.16
Reduced stack parameter[c]:	0.14
Description:	energy-efficient basement active solar attached vertical greenhouse vapor barrier

Predicted and Measured Infiltration[d]				
Stack	Wind	Total Predicted	Measured	Difference
43	81	92	82	12%
44	69	82	72	14%
44	81	92	98	-6%
44	92	102	98	4%
45	92	103	89	16%

---

1) SI units

2) cm^2

3) $m/s/K^{1/2}$

4) m^3/hr

Table 5 : Test results for test site #5

Site ID:	R-10
Reference No.	3
House Volume[a]	233
No. of Stories	1
Leakage Area[b]	330
Floor Area[a]	97
Terrain factor	0.85
Shielding Class	3
Reduced wind parameter:	0.15
Reduced stack parameter[c]:	0.09
Description:	ranch style baseboard electric-resistance heating

Predicted and Measured Infiltration[d]				
Stack	Wind	Total Predicted	Measured	Difference
50	80	94	105	-10%

1) SI units

2) cm^2

3) $m/s/K^{1/2}$

4) m^3/hr

Table 6 : Test results for test site #6

Site ID:	T1
Reference No.	12
House Volume[a]	337
No. of Stories	1
Leakage Area[b]	330
Floor Area[a]	77
Terrain factor	0.77
Shielding Class	3
Reduced wind parameter:	0.14
Reduced stack parameter[c]:	0.10
Description:	basement fireplace forced-air

Predicted and Measured Infiltration[d]				
Stack	Wind	Total Predicted	Measured	Difference
64	23	68	74	-8%
12	45	46	54	-15%
51	67	84	78	8%

1) SI units

2) cm^2

3) $m/s/K^{1/2}$

4) m^3/hr

Table 7 : Test results for test site #7

Site ID:	T2
Reference No.	12
House Volume[a]	433
No. of Stories	1
Leakage Area[b]	680
Floor Area[a]	100
Terrain factor	0.77
Shielding Class	3
Reduced wind parameter:	0.17
Reduced stack parameter[c]:	0.11
Description:	basement fireplace forced-air

Predicted and Measured Infiltration[d]				
Stack	Wind	Total Predicted	Measured	Difference
115	112	161	169	-5%
28	29	40	48	-17%
154	196	249	199	25%

1) SI units

2) cm^2

3) $m/s/K^{1/2}$

4) m^3/hr

Table 8 : Test results for test site #8

Site ID:	HAVEN
Reference No.	2
House Volume[a]	230
No. of Stories	1
Leakage Area[b]	770
Floor Area[a]	100
Terrain factor	0.71
Shielding Class	5
Reduced wind parameter:	0.07
Reduced stack parameter[c]:	0.10
Description:	crawl space forced-air fireplace

Predicted and Measured Infiltration[d]				
Stack	Wind	Total Predicted	Measured	Difference
55	39	67	49	37%
92	58	109	71	54%
88	78	117	85	38%

1) SI units

2) cm^2

3) $m/s/K^{1/2}$

4) m^3/hr

Table 9 : Test results for test site #9

Site ID:	PURDUE
Reference No.	2
House Volume[a]	240
No. of Stories	1
Leakage Area[b]	855
Floor Area[a]	93
Terrain factor	0.62
Shielding Class	4
Reduced wind parameter:	0.11
Reduced stack parameter[c]:	0.11
Description:	crawl space forced-air fireplace nonrectangular floor plan

Predicted and Measured Infiltration[d]				
Stack	Wind	Total Predicted	Measured	Difference
102	67	122	120	2%
102	67	122	125	-2%
102	136	170	154	10%
107	170	200	166	20%

1) SI units

2) cm^2

3) $m/s/K^{1/2}$

4) m^3/hr

Table 10 : Test results for test site #10

Site ID:	NEILSON
Reference No.	2
House Volume[a]	250
No. of Stories	1
Leakage Area[b]	1275
Floor Area[a]	96
Terrain factor	0.62
Shielding Class	3
Reduced wind parameter:	0.15
Reduced stack parameter[c]	0.12
Description:	crawl space floor furnace fireplace — undampered nonrectangular floor plan

Predicted and Measured Infiltration[d]				
Stack	Wind	Total Predicted	Measured	Difference
123	138	185	175	6%
135	138	193	160	21%
110	69	130	185	-30%
123	69	141	340	-59%

1) SI units

2) cm^2

3) $m/s/K^{1/2}$

4) m^3/hr

Table 11 : Test results for test site #11

Site ID:	V1
Reference No.	2
House Volume[a]	270
No. of Stories	1
Leakage Area[b]	560
Floor Area[a]	104
Terrain factor	0.81
Shielding Class	3
Reduced wind parameter:	0.18
Reduced stack parameter[c]:	0.12
Description:	energy-efficient active solar slab on grade vapor barrier wood stove

Predicted and Measured Infiltration[d]				
Stack	Wind	Total Predicted	Measured	Difference
59	76	96	84	-5%
64	80	102	89	15%

---

1) SI units

2) cm^2

3) $m/s/K^{1/2}$

4) m^3/hr

Table 12 : Test results for test site #12

Site ID:	V2
Reference No.	2
House Volume[a]	270
No. of Stories	1
Leakage Area[b]	630
Floor Area[a]	104
Terrain factor	0.81
Shielding Class	4
Reduced wind parameter:	0.14
Reduced stack parameter[c]:	0.12
Description:	energy-efficient active solar slab on grade vapor barrier wood stove

Predicted and Measured Infiltration[d]				
Stack	Wind	Total Predicted	Measured	Difference
82	143	165	173	14%
61	67	90	78	15%

1) SI units

2) cm^2

3) $m/s/K^{1/2}$

4) m^3/hr

Table 13 : Test results for test site #13

Site ID:	FELS
Reference No.	1
House Volume[a]	470
No. of Stories	2
Leakage Area[b]	1480
Floor Area[a]	152
Terrain factor	0.84
Shielding Class	5
Reduced wind parameter:	0.08
Reduced stack parameter[c]:	0.13
Description:	basement forced-air

Predicted and Measured Infiltration[d]				
Stack	Wind	Total Predicted	Measured	Difference
277	170	325	355	-8%
183	426	464	320	45%

1) SI units
2) cm^2
3) $m/s/K^{1/2}$
4) m^3/hr

Table 14 : Test results for test site #14

Site ID:	SAN CARLOS
Reference No.	2
House Volume[a]	145
No. of Stories	1
Leakage Area[b]	845
Floor Area[a]	58
Terrain factor	0.81
Shielding Class	4
Reduced wind parameter:	0.15
Reduced stack parameter[c]:	0.11
Description:	crawl space floor furnace fireplace — undampered

Predicted and Measured Infiltration[d]				
Stack	Wind	Total Predicted	Measured	Difference
0	76	76	149	-49%
47	49	68	116	-41%
47	89	101	90	12%
0	93	93	107	-13%

1) SI units

2) cm^2

3) $m/s/K^{1/2}$

4) m^3/hr

Table 15 : Test results for test site #15

Site ID:	SOUTHAMPTON
Reference No.	2
House Volume[a]	1000
No. of Stories	3
Leakage Area[b]	1640
Floor Area[a]	370
Terrain factor	0.90
Shielding Class	3
Reduced wind parameter:	0.20
Reduced stack parameter[c]:	0.16
Description:	basement and crawl space fireplace forced air nonrectangular floor plan

Predicted and Measured Infiltration[d]				
Stack	Wind	Total Predicted	Measured	Difference
94	124	156	250	38%
188	124	255	310	-18%
94	124	156	190	-18%

1) SI units

2) cm^2

3) $m/s/K^{1/2}$

4) m^3/hr

REFERENCES

1. J.E. Janssen, "Calculating Infiltration An Examination of Handbook Models," ASHRAE Trans.86:II (1980).

2. D.R. Bahnfleth, D.T. Moseley, and W.S. Harris, "Measurement of Infiltration in Two Residences," ASHRAE Trans., 63, 439-452, (1957).

3. J.B. Dick, and D.A. Thomas, "Ventilation Research in Occupied Houses," J. Inst. Heat. Vent. Eng., 19, 306-332, 1951.

4. N. Malik, "Field Studies of Dependence of Air Infiltration on Outside Temperature and Wind," Energy and Buildings, 1, 281-292, 1978.

5. D.T. Grimsrud, M.H. Sherman, R.C. Diamond, P.E. Condon, and A.H. Rosenfeld, "Infiltration-Pressurization Correlations: Detailed Measurements on a California House," ASHRAE Trans., 85, 1:851-865, (1979). Lawrence Berkeley Laboratory report LBL-7824 (1978).

6. R.E. Akins, J.A. Peterka, and J.E. Cermak, "Average Pressure Coefficients for Rectangular Buildings," Proceedings of the Fifth Int. Conf. Wind Engineering, Boulder, Colorado, July 1979.

7. European Convention for Constructional Steelwork, "Recommendations for the Calculation of Wind Effects on Buildings and Structures", Technical General Secretariat, Brussels, Belgium, September 1978.

8. M.H. Sherman, D.T. Grimsrud, R.C. Diamond, "Infiltration-Pressurization Correlation: Surface Pressures and Terrain Effects," ASHRAE Trans. 85-II, (1979) Lawrence Berkeley Laboratory report LBL-8785 (1979).

9. D.T. Grimsrud, M.H. Sherman, A.K. Blomsterberg, and A.H. Rosenfeld, Infiltration and Air Leakage Comparisons: Conventional and Energy Efficient Housing Designs, Lawrence Berkeley Laboratory report, LBL-9157 (1979). Presented at the International Conference on Energy Use Management, Los Angeles, October 1979.

10. Johns-Manville Research and Development Center, "Demonstration of Energy Conservation through Reduction of Air Infiltration in Electrically Heated Houses," RP 1351-1, (1979).

11. G.T. Tamura, "The Calculation of House Infiltration Rates," ASHRAE Trans, 85, Part 1 p. 58-71, (1979).

12. M.P. Modera and M.H. Sherman, "The Calculation of Air Flow through Fossil Fueled Fired Flues," Unpublished.

13. S. Kim, K.C. Mehta, Full-Scale Measurements on a Flat Roof Area, in Proceedings of the Fifth Int. Conf. Wind Engineering, Boulder, Colorado, July 1979.

14. Harrje, D.T., Blomsterberg, A.K., and Persily, A., Reduction of Air Infiltration due to Window and Door Retrofits in an Older Home, Princeton University, Center for Environmental Studies, Princeton, NJ, Report No. 85, 1979.

15. Grimsrud, D.T., Sherman, M.H., Blomsterberg, A.K., and Rosenfeld, A.H., Infiltration and Air Leakage Comparisons: Conventional and Energy Efficient Housing Designs Lawrence Berkeley Laboratory report, LBL-9157, 1979. Presented at the International Conference on Energy Use Management, Los Angeles, October 1979.

16. Johns-Manville Research and Development Center opcit, Demonstration of Energy Conservation through Reduction of Air Infiltration in Electrically Heated Houses, RP 1351-1, 1979.

17. Tamura, G.T., "The Calculation of House Infiltration Rates," ASHRAE Trans., 85, 1:58-71, 1979.

FIGURE CAPTIONS

FIG. 1 The leakage area for each of the 15 measured sites.

FIG. 2 The correlation of infiltration measured using a tracer gas technique and using the model presented in this report. Dashed lines represent raw measurement error limits. Only data under $150m^3/hr$ is shown.

FIG. 3 The correlation of infiltration measured using a tracer gas technique and using the model presented in this report. Dashed lines represent raw measurement error limits. Only data over $100m^3/hr$ is shown.

FIG. 4 The percentage disagreement between tracer measurements and predictive technique vs leakage area for each site. Solid points are individual measurements; open points with error bars represent site average. Composite for all sites is shown at right.

FIG. 5 The stack parameter versus neutral level.

FIG. 6 The neutral level versus the ceiling/floor leakage difference.

FIG. 7 The stack parameters versus the ceiling/floor leakage difference.

FIG. 8 A graphical method for calculating infiltration from weather data.

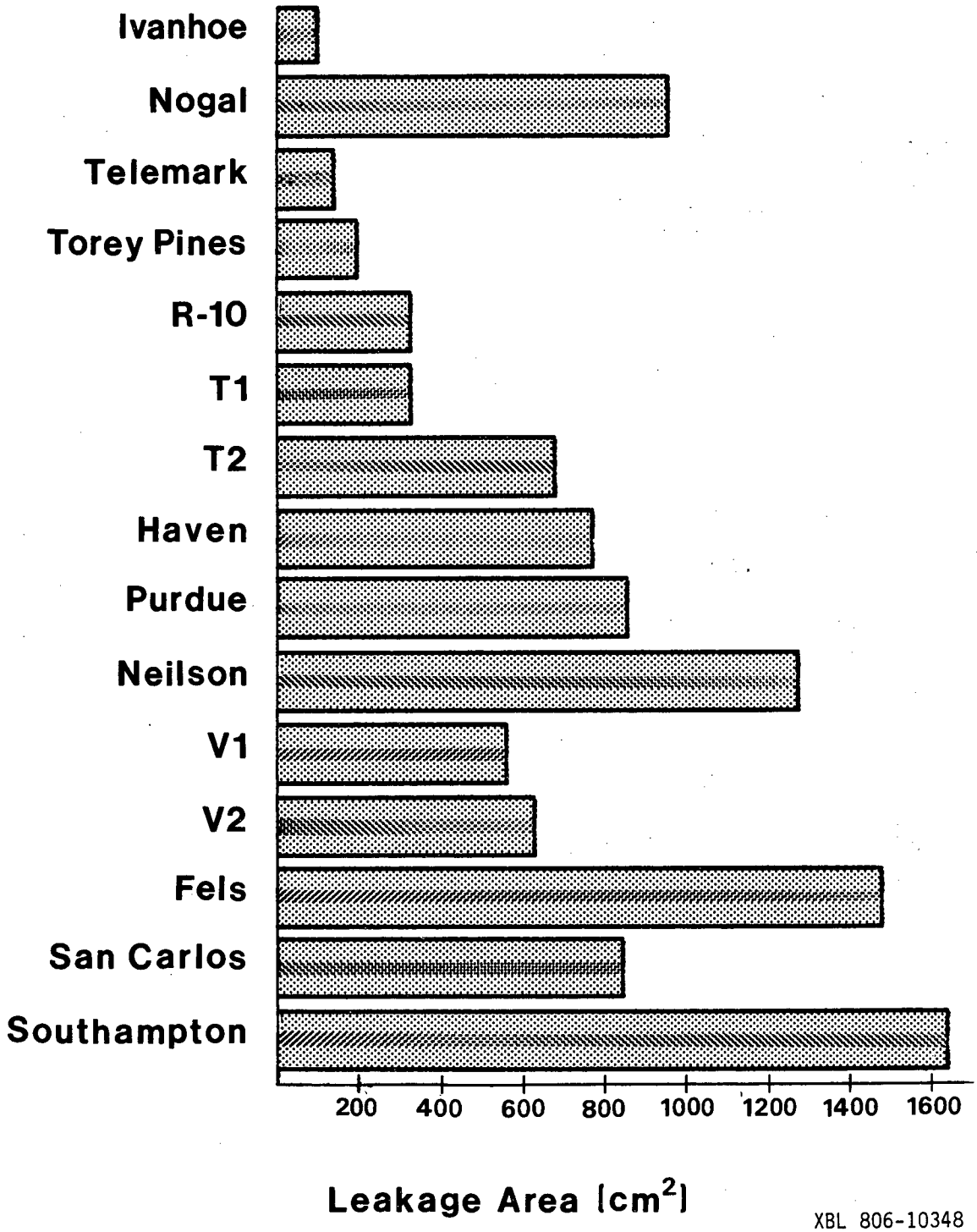

FIG. 1 The leakage area for each of the 15 measured sites.

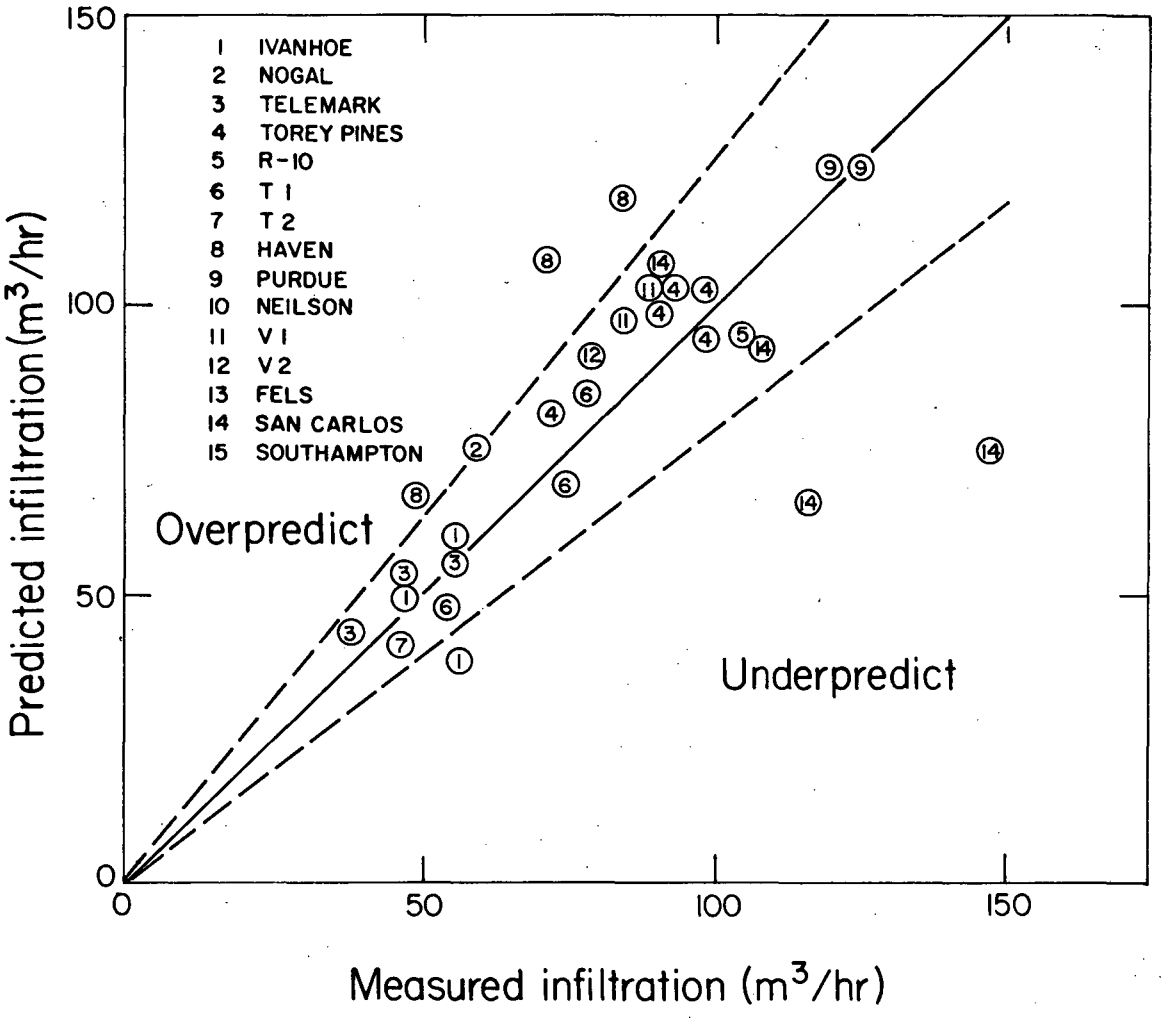

XBL 805-907

FIG. 2 The correlation of infiltration measured using a tracer gas technique and using the model presented in this report.

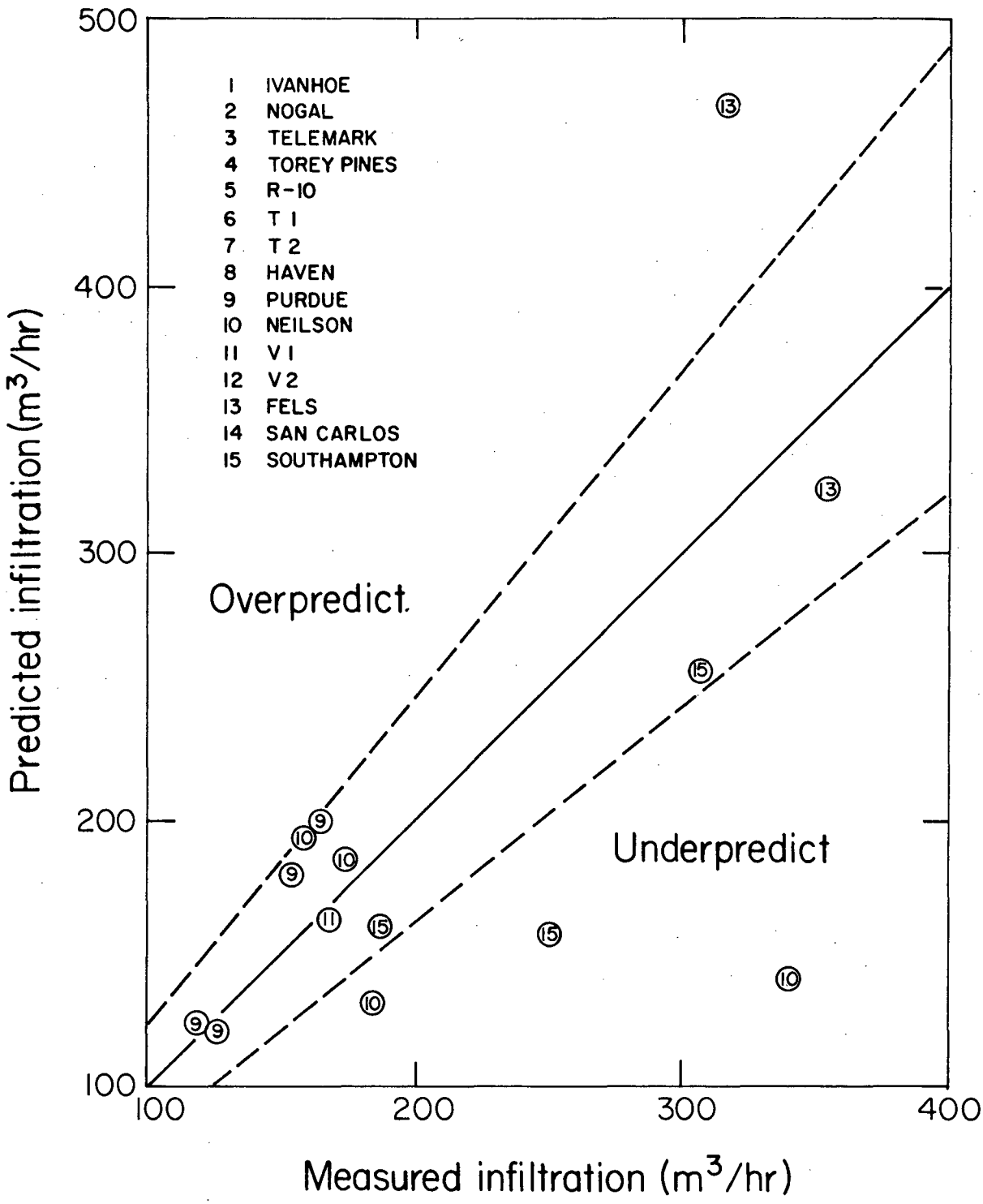

XBL 805-908

FIG. 3 The correlation of infiltration measured using a tracer gas technique and using the model presented in this report.

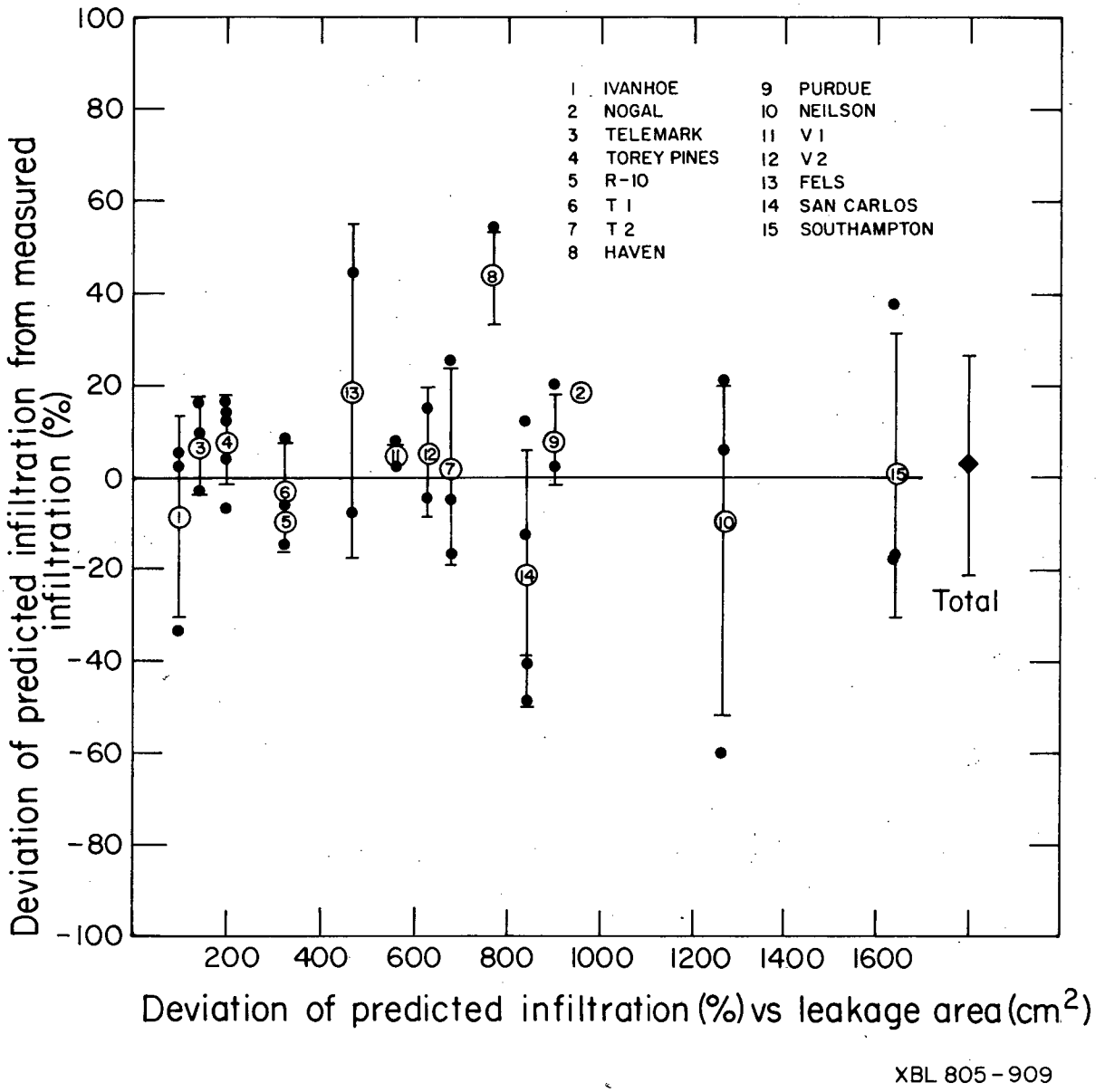

FIG. 4 The percentage disagreement between tracer measurements and predictive technique vs leakage area for each site.

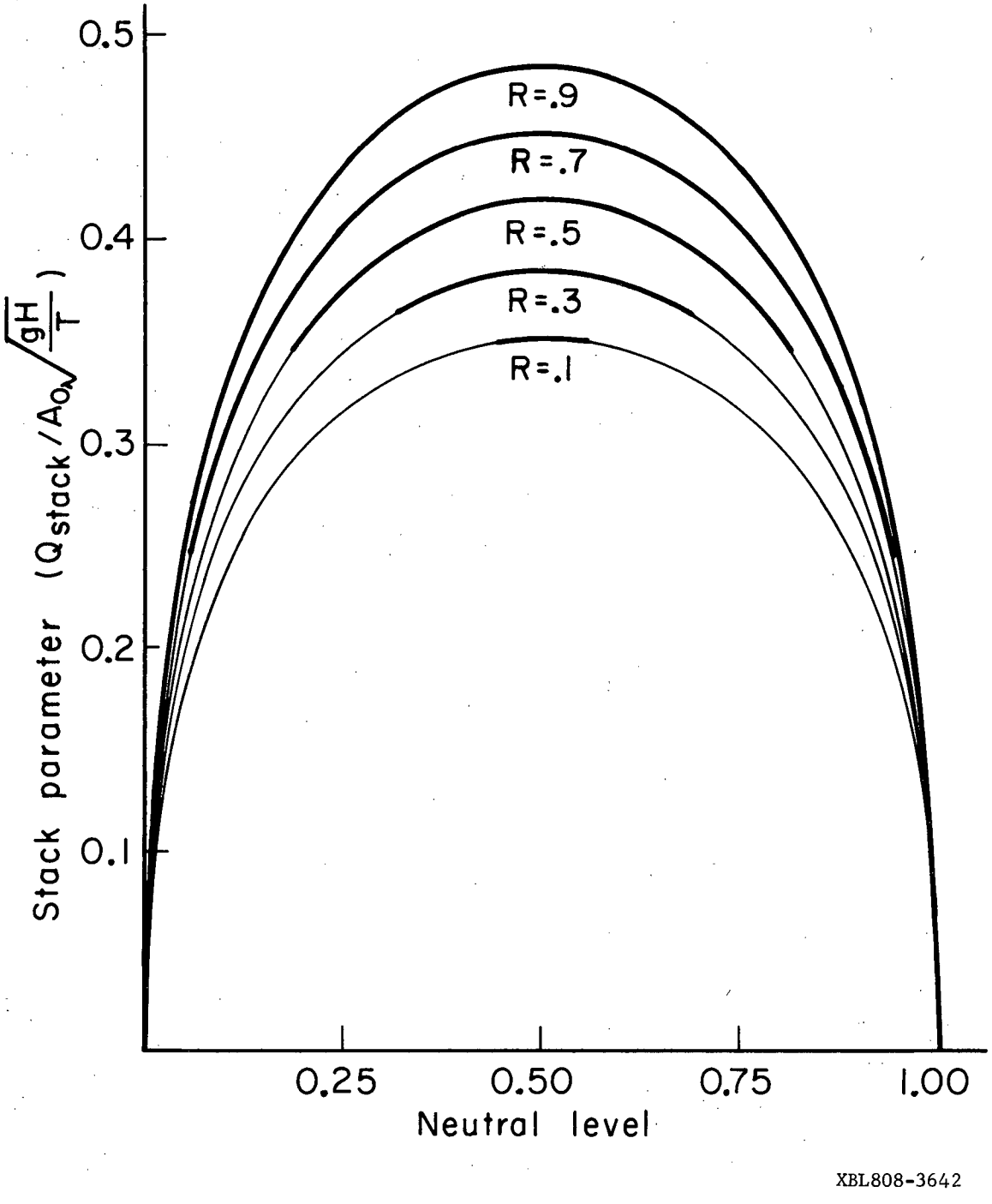

FIG. 5 The stack parameter versus neutral level.

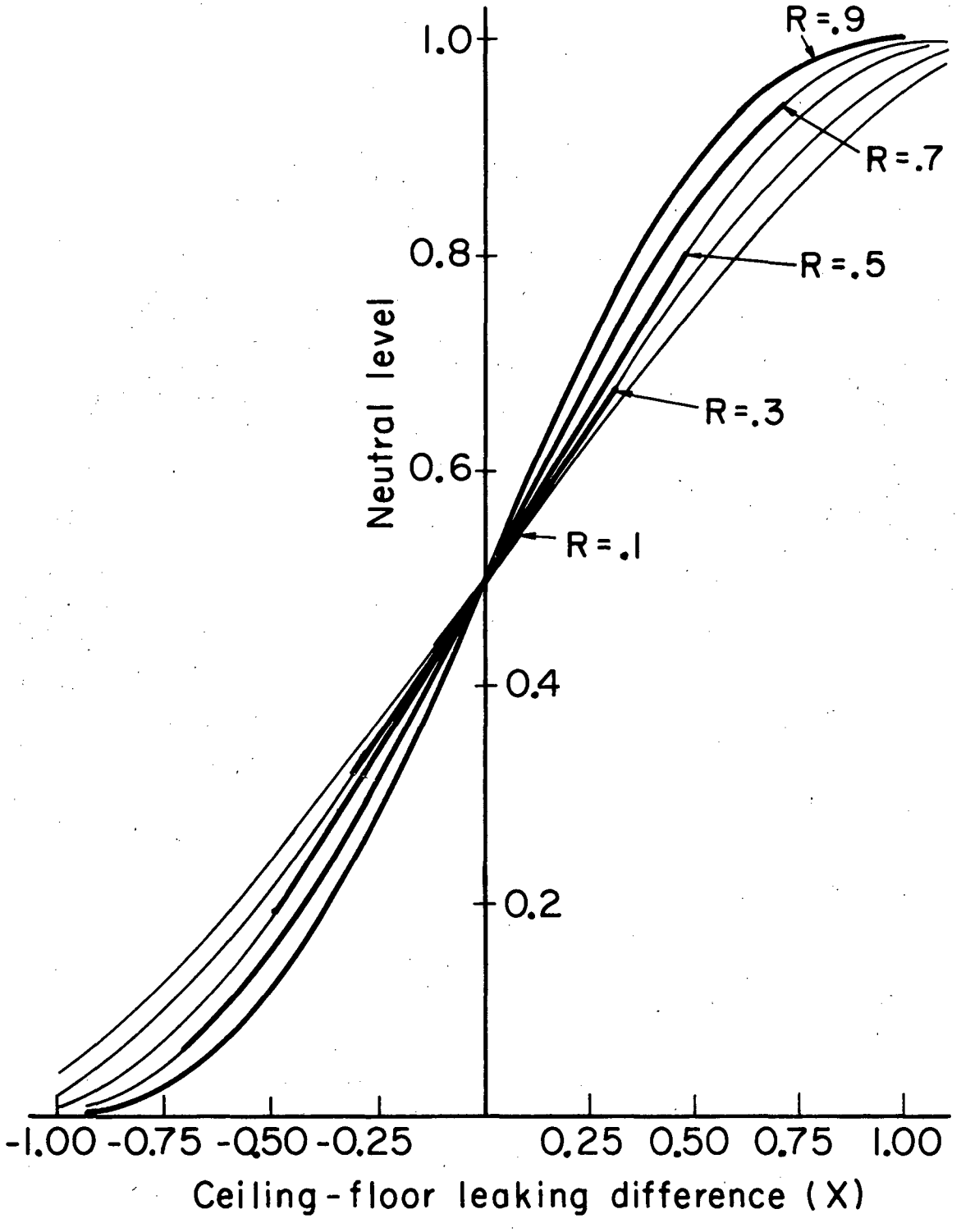

XBL808-3640

FIG. 6 The neutral level versus the ceiling/floor leakage difference.

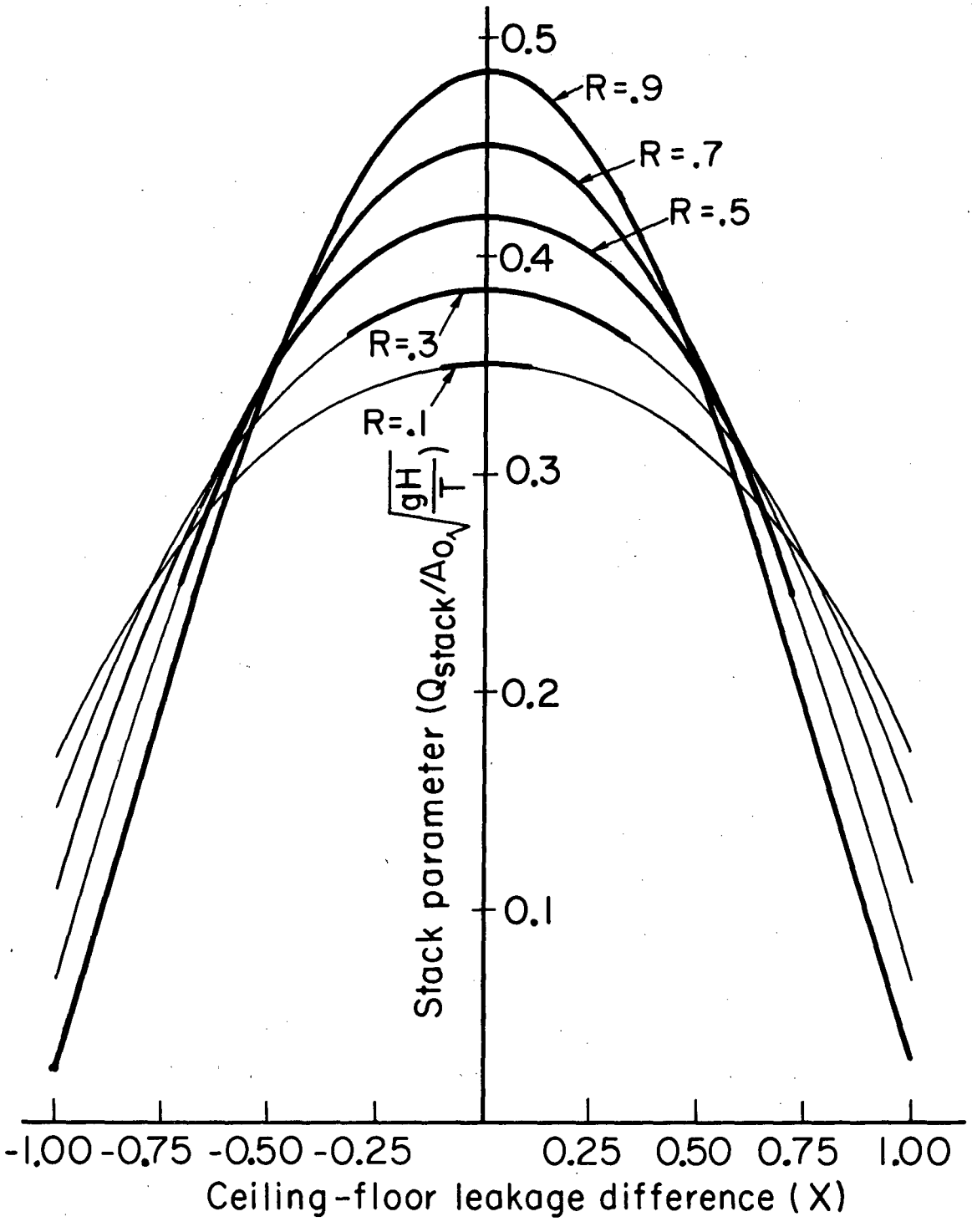

XBL808-3641

FIG. 7 The stack parameters versus the ceiling/floor leakage difference.

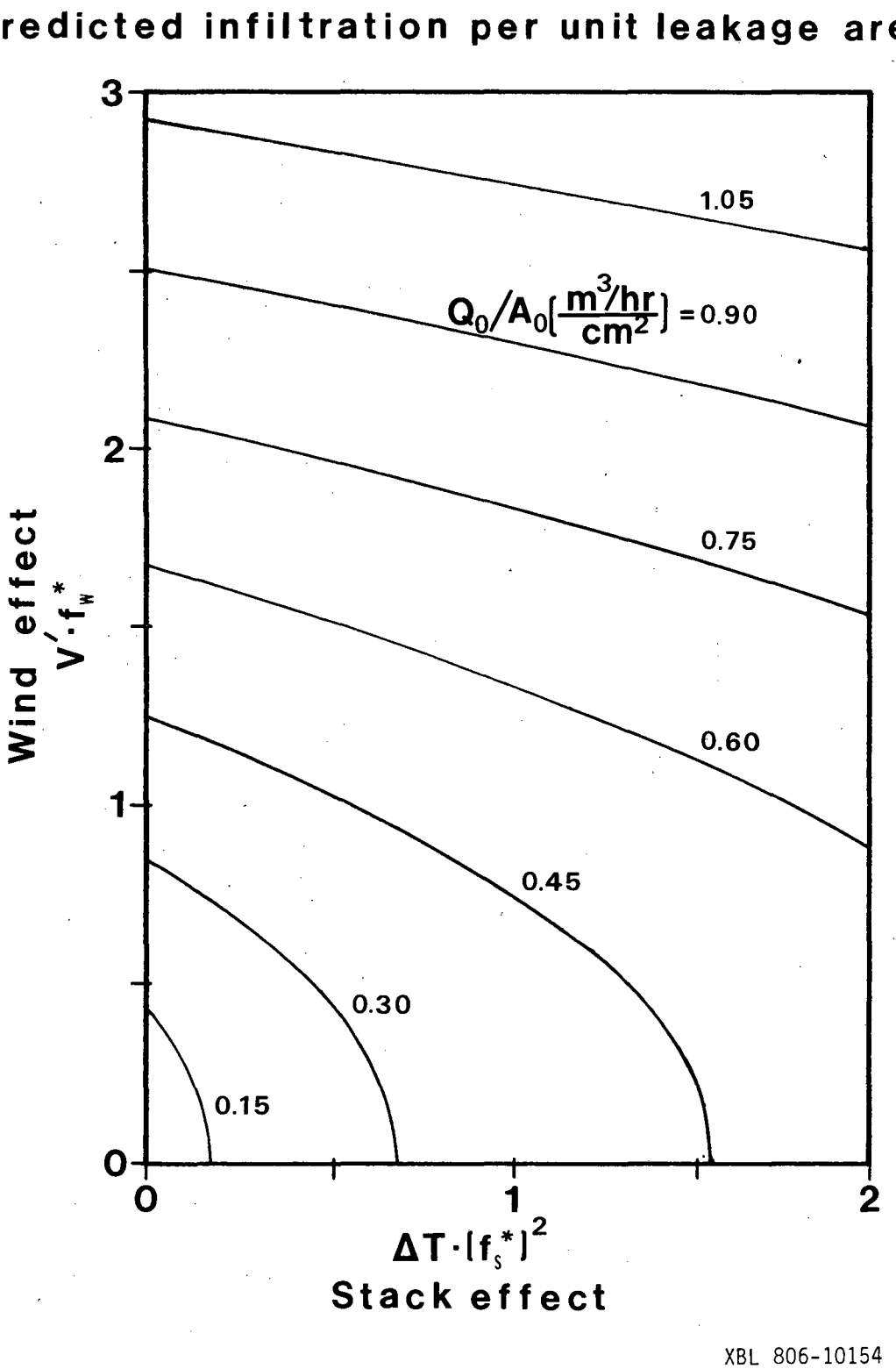

FIG. 8 A graphical method for calculating infiltration from weather data.

This report was done with support from the Department of Energy. Any conclusions or opinions expressed in this report represent solely those of the author(s) and not necessarily those of The Regents of the University of California, the Lawrence Berkeley Laboratory or the Department of Energy.

Reference to a company or product name does not imply approval or recommendation of the product by the University of California or the U.S. Department of Energy to the exclusion of others that may be suitable.

TECHNICAL INFORMATION DEPARTMENT
LAWRENCE BERKELEY LABORATORY
UNIVERSITY OF CALIFORNIA
BERKELEY, CALIFORNIA 94720